



# Repetitive Sampling Control Chart for Gamma Distribution in Uncertain Environments

Zainalabideen Al-Husseini<sup>1</sup>, Khudhayr A. Rashedi<sup>2</sup>, Muhammad Aslam<sup>3</sup>

<sup>1</sup>Department of Accounting, College of Administrative Sciences, Al-Mustaqbal University, 51001, Babylon, Iraq

zainalabden.aboad@uomus.edu.iq

<sup>2</sup>Department of Mathematics, College of Science, University of Ha'il, Hail, Saudi Arabia

k.rashedi@uoh.edu.sa

<sup>3</sup>Department of Statistics, Faculty of Science, King Abdulaziz University, Jeddah, 21551, Saudi Arabia;

aslam\_ravian@hotmail.com

**Abstract:** This paper introduces an innovative control chart customized for the gamma distribution, specifically crafted to handle uncertain conditions through repetitive sampling. The control chart's coefficients, along with the probabilities of remaining in control or detecting a shift, and the average run lengths, were derived by assuming the symmetrical behavior typical of the normal distribution, using the neutrosophic interval method. The performance of this chart was evaluated by assessing average run lengths under various uncertain process conditions. The chart's efficacy in identifying both minor and major process shifts was investigated. This study also provides a comparison between the newly proposed chart and existing ones. To demonstrate its practical utility, an example from the healthcare sector is provided. Both simulation results and this practical example confirm that the new control chart is effective in swiftly identifying deviations in processes, making it a valuable tool for managing uncertainty.

**Keywords:** Control chart, shift; simulation; imprecise data; industrial process

## 1 Introduction

Control charts are widely recognized as one of the most potent tools in statistical process control, with applications spanning various industries. Suman and Prajapati [1] investigated their use in healthcare, Zaman, Lee, and Riaz [2] applied them to wind turbine monitoring, and Hossain et al. [3] employed them for overseeing the glass fiber process. The efficacy of a control chart is gauged by its responsiveness to changes in its parameters. Two types of changes are acknowledged: common changes (or common causes), which are natural and non-threatening, and special changes (or special causes), which can significantly affect the quality characteristic of interest Montgomery [4] A crucial feature of any control chart is its ability to swiftly detect special causes of variation, thereby preventing the production of defective items and avoiding substantial losses Ahmad, Aslam, and Jun [5]. The concept of the control chart was introduced by Walter A. Shewhart [6], and researchers have since been endeavoring to develop robust control charts. Variable control

charts are used when data comes from measurement processes, while attribute control charts are for data obtained from counting processes, see Abid et al.[7]. proposed a control chart for healthcare monitoring, Aslam and Raza [8] designed one for the process capability index, and Nazir et al. [9] enhanced control charts for industrial processes. Saghir, Ahmad, and Aslam [10] developed charts for modified gamma data, incorporating auxiliary information and repetitive sampling.

Repetitive sampling schemes (RSS) have gained prominence in statistical process control, attracting considerable research attention over the past two decades. Initially introduced by Sherman [11] for attribute acceptance sampling plans, RSS has been extended to normal and log-normal distributions by Balamurali et al. [12] and Bhaumik and Gibbons [13]. The efficiency of RSS lies between single sampling and probability-to-ratio sampling schemes Balamurali et al [12]. Ahmad, Aslam, and Jun [14] developed Shewhart X-bar control charts using RSS for monitoring process capability indices and coal quality, while Azam et al. [15] developed plans for exponentially weighted moving average regression estimators. The gamma distribution, a family of two-parameter continuous probability distributions, is especially useful in quality control when the shape of the data is unknown or non-normal Al-Oraini and Rahim [16] and Stoumbos and Reynolds Jr [17]. It is particularly effective for modeling waiting times and failure times in systems or processes Aksoy [18] Saghir et al [19]. For skewed data, the gamma distribution serves as a better approximation than the normal distribution Aslam et al. [20]. Bhaumik and Gibbons [13]. Numerous control charts have been developed for monitoring skewed statistics, such as those by Jearkpaporn et al. [21] for mean shifts, Zhang et al. [22] for random shift models, F. L. Chen and Yeh [23] for non-normal distributions, and Gonzalez and Viles [24] for r-charts under the gamma distribution.

Traditionally, control charts assume clear, precise observations. However, real-world data can often be unclear or fuzzy. Bradshaw Jr [25] developed control charts using fuzzy set theory, while Williams and Zigli [26] proposed charts for the service industry using fuzzy logic. Other notable contributions include procedures for linguistic data Taleb and Limam [27], fuzzy control charts for linguistic data (Gülbay, Kahraman, and Ruan [28], and Poisson-based control charts for wafer defects Hsieh et al. [29]. Neutrosophic logic, an extension of the fuzzy logic proposed by Smarandache (1998), addresses indeterminacy, which fuzzy logic cannot. Neutrosophic statistics generalize classical statistics for indeterminate environments. Applications include scale effect and anisotropy analysis for rock joint roughness Chen et al. [30], sampling plans for process loss consideration Aslam [31], and control charts for multiple manufacturing lines Aslam and Raza [8]. Average run length (ARL) is a common evaluation tool for control charts, defined as the average number of samples before an out-of-control condition is detected Montgomery [4]. Neutrosophic ARL (NARL) should be high for in-control processes and low for out-of-control processes, ensuring quick detection of issues Molnau et al. [32], Schaffer and Kim [33], Knoth [34], Li et al. [35] Chananet et al. [36] and Phanyaem et al. [37].

This article develops a control chart using the gamma distribution and repetitive sampling for indeterminate environments, aiming to provide an efficient monitoring scheme. To the author's knowledge, no prior work has addressed this combination. The paper is structured as follows: Section 2 introduces the neutrosophic gamma distribution, Section 3 details the design of the proposed chart, including NARL tables and a simulation study. Section 4 compares the proposed

chart with existing ones, and Section 5 provides a practical example. The conclusion and future research directions are presented in the last section.

## 2 Gamma Distribution under Neutrosophic Statistics

Suppose  $T_N \in [T_L, T_U]$  be imprecise failure time and modeled using neutrosophic gamma distribution (NGD) with scale parameter  $b_N \in [b_L, b_U]$  and shape parameter  $a_N \in [a_L, a_U]$ , respectively. The neutrosophic probability density function (npdf) is expressed by

$$f(t_N) = \frac{b_N^{a_N}}{\Gamma(a_N)} t_N^{a_N-1} e^{-b_N t_N}; t_N, a_N, b_N > 0; a_N \in [a_L, a_U], b_N \in [b_L, b_U] \quad (1)$$

where  $\Gamma(x)$  shows the neutrosophic gamma function; for further details, refer to Aslam et al [38]. The corresponding neutrosophic cumulative distribution (NCD) is given by

$$P(T_N \leq t_N) = 1 - \sum_{j=1}^{a_N-1} \frac{e^{-\frac{t_N}{b_N}} (\frac{t_N}{b_N})^j}{j!}; T_N \in [T_L, T_U], a_N \in [a_L, a_U], b_N \in [b_L, b_U] \quad (2)$$

It is important to mention that within classical statistics, the NGD is an extension of the conventional gamma distribution with the following mean and variance

$$\mu_N = \frac{a_N}{b_N}; a_N \in [a_L, a_U], b_N \in [b_L, b_U] \quad (3)$$

and

$$\sigma_N^2 = \frac{a_N}{b_N^2}; a_N \in [a_L, a_U], b_N \in [b_L, b_U] \quad (4)$$

This distribution is developed using the approximation by [39] as  $T_N^* = T_N^{1/3}; T_N \in [T_L, T_U]$  with the following mean and variance. For more details on neutrosophic distribution, refer to Peng and Dai [40], Peng and Dai [41], Aslam and Raza [8] and Aslam [31].

$$\mu_{T_N^*} = \frac{b_N^{1/3} \Gamma(a_N + 1/3)}{\Gamma(a_N)}; a_N \in [a_L, a_U], b_N \in [b_L, b_U] \quad (5)$$

and

$$\sigma_{T_N^*}^2 = \frac{b_N^{2/3} \Gamma(a_N + 2/3)}{\Gamma(a_N)} - \left( \frac{b_N^{1/3} \Gamma(a_N + 1/3)}{\Gamma(a_N)} \right)^2; a_N \in [a_L, a_U], b_N \in [b_L, b_U] \quad (6)$$

## 3. The Propose Chart

Following Wilson and Hilferty [39], the transformed variable  $T_N^* = T_N^{1/3}; T_N \in [T_L, T_U]$  retains the symmetry property of the neutrosophic normal distribution. We propose the following control chart under the uncertainty when the quality characteristic follows the NGD. The development of the neutrosophic control chart involves the following two steps:

1. Calculate  $T_N^* = T_N^{1/3}$  using the data.

2. Declare the process out-of-control if  $T_N^* \geq UCL_{1N}$  or  $T_N^* \leq LCL_{1N}$ . The process is considered out-of-control, otherwise.

The proposed neutrosophic control chart, extends the control chart developed by Sheu and Lin [42] in classical statistics. When applied to crisp, complete, or certain observations, the proposed chart simplifies to the Sheu and Lin [42] control chart. Suppose  $b_{0N} \in [b_{0L}, b_{0U}]$  be in-control scale parameter with the following control limits

$$LCL_{1N} = \mu_{T_N^*} - k_{1N} \sigma_{T_N^*} = \frac{b_{0N}^{1/3} \Gamma(a_N + \frac{1}{3})}{\Gamma(a_N)} - k_{1N} \sqrt{\frac{b_{0N}^{2/3} \Gamma(a_N + 2/3)}{\Gamma(a_N)} - \mu_{T_N^*}^2} \tag{7}$$

$$LCL_{2N} = \mu_{T_N^*} - k_{2N} \sigma_{T_N^*} = \frac{b_{0N}^{1/3} \Gamma(a_N + \frac{1}{3})}{\Gamma(a_N)} - k_{2N} \sqrt{\frac{b_{0N}^{2/3} \Gamma(a_N + 2/3)}{\Gamma(a_N)} - \mu_{T_N^*}^2} \tag{8}$$

$$UCL_{1N} = \mu_{T_N^*} + k_{1N} \sigma_{T_N^*} = \frac{b_{0N}^{1/3} \Gamma(a_N + 1/3)}{\Gamma(a_N)} + k_{1N} \sqrt{\frac{b_{0N}^{2/3} \Gamma(a_N + 2/3)}{\Gamma(a_N)} - \mu_{T_N^*}^2} \tag{9}$$

$$UCL_{2N} = \mu_{T_N^*} + k_{2N} \sigma_{T_N^*} = \frac{b_{0N}^{1/3} \Gamma(a_N + 1/3)}{\Gamma(a_N)} + k_{2N} \sqrt{\frac{b_{0N}^{2/3} \Gamma(a_N + 2/3)}{\Gamma(a_N)} - \mu_{T_N^*}^2} \tag{10}$$

where  $k_{1N} \in [k_{1L}, k_{1U}]$  and  $k_{2N} \in [k_{2L}, k_{2U}]$  represent the neutrosophic control limit coefficients. Additionally, we define

$$LL_{1N} = \left[ \frac{\Gamma(a_N + 1/3)}{\Gamma(a_N)} - k_{1N} \sqrt{\frac{\Gamma(a_N + 2/3)}{\Gamma(a_N)} - \left(\frac{\Gamma(a_N + 1/3)}{\Gamma(a_N)}\right)^2} \right]$$

$$LL_{2N} = \left[ \frac{\Gamma(a_N + 1/3)}{\Gamma(a_N)} - k_{2N} \sqrt{\frac{\Gamma(a_N + 2/3)}{\Gamma(a_N)} - \left(\frac{\Gamma(a_N + 1/3)}{\Gamma(a_N)}\right)^2} \right]$$

$$UL_{1N} = \left[ \frac{\Gamma(a_N + 1/3)}{\Gamma(a_N)} + k_{1N} \sqrt{\frac{\Gamma(a_N + 2/3)}{\Gamma(a_N)} - \left(\frac{\Gamma(a_N + 1/3)}{\Gamma(a_N)}\right)^2} \right]$$

$$UL_{2N} = \left[ \frac{\Gamma(a_N + 1/3)}{\Gamma(a_N)} + k_{2N} \sqrt{\frac{\Gamma(a_N + 2/3)}{\Gamma(a_N)} - \left(\frac{\Gamma(a_N + 1/3)}{\Gamma(a_N)}\right)^2} \right]$$

Thus, the neutrosophic control limits can be expressed as follows:

$$LCL_{1N} = b_{0N}^{1/3} LL_{1N} \tag{11}$$

$$LCL_{2N} = b_{0N}^{1/3} LL_{2N} \tag{12}$$

$$UCL_{1N} = b_{0N}^{1/3} UL_{1N} \tag{13}$$

$$UCL_{2N} = b_{0N}^{1/3} UL_{2N} \tag{14}$$

For the shifted process, the necessary equations are given by

$$P_{out,N}^0 = P(T_N^* < LCL_{1N} | b_N = b_{0N}) + P(T_N^* > UCL_{1N} | b_N = b_{0N}) \tag{15}$$

or

$$P_{out,N}^0 = 1 - \sum_{j=1}^{a_N-1} \frac{e^{-LL_{1N}^3} (LL_{1N}^3)^j}{j!} + \sum_{j=1}^{a_N-1} \frac{e^{-UL_{1N}^3} (UL_{1N}^3)^j}{j!} \tag{16}$$

$$P_{rep,N}^0 = P(LCL_{1N} < T_N^* < LCL_{2N} | b_N = b_{0N}) + P(UCL_{1N} < T_N^* < UCL_{2N} | b_N = b_{0N}) \tag{17}$$

$$P_{rep,N}^0 = \sum_{j=1}^{a_N-1} \frac{e^{-UL_{2N}^3}(UL_{2N}^3)^j}{j!} - \sum_{j=1}^{a_N-1} \frac{e^{-UL_{1N}^3}(UL_{1N}^3)^j}{j!} + \sum_{j=1}^{a_N-1} \frac{e^{-LL_{1N}^3}(LL_{1N}^3)^j}{j!} - \sum_{j=1}^{a_N-1} \frac{e^{-LL_{2N}^3}(LL_{2N}^3)^j}{j!} \tag{18}$$

$$P_{out}^0 = \frac{P_{out,N}^0}{1 - P_{rep,N}^0} \tag{19}$$

The Neutrosophic Average Run Length (NARL) defined as

$$ARL_{0N} = \frac{1}{P_{out}^0}; ARL_{0N} \in [ARL_{0L}, ARL_{0U}] \tag{21}$$

If a shift occurs in the process, it moves from the target  $b_{0N} \in [b_{0L}, b_{0U}]$  to  $b_{1N} = cb_{0N}$ ;  $b_{1N} \in [b_{1L}, b_{1U}]$ , where the constant  $c$  represents the magnitude of the shift. The necessary equations are given below

$$P_{out,N}^1 = P(T_N^* < LCL_{1N} | b_N = cb_{0N}) + P(T_N^* > UCL_{1N} | b_N = cb_{0N}) \tag{22}$$

or

$$P_{out,N}^1 = 1 - \sum_{j=1}^{a_N-1} \frac{e^{-\frac{LL_{1N}^3}{c}}(\frac{LL_{1N}^3}{c})^j}{j!} + \sum_{j=1}^{a_N-1} \frac{e^{-\frac{UL_{1N}^3}{c}}(\frac{UL_{1N}^3}{c})^j}{j!} \tag{23}$$

$$P_{rep,N}^1 = P(LCL_{1N} < T_N^* < LCL_{2N} | b_N = cb_{0N}) + P(UCL_{1N} < T_N^* < UCL_{2N} | b_N = cb_{0N}) \tag{24}$$

$$P_{rep,N}^1 = \sum_{j=1}^{a_N-1} \frac{e^{-\frac{UL_{2N}^3}{c}}(\frac{UL_{2N}^3}{c})^j}{j!} - \sum_{j=1}^{a_N-1} \frac{e^{-\frac{UL_{1N}^3}{c}}(\frac{UL_{1N}^3}{c})^j}{j!} + \sum_{j=1}^{a_N-1} \frac{e^{-\frac{LL_{1N}^3}{c}}(\frac{LL_{1N}^3}{c})^j}{j!} - \sum_{j=1}^{a_N-1} \frac{e^{-\frac{LL_{2N}^3}{c}}(\frac{LL_{2N}^3}{c})^j}{j!} \tag{25}$$

$$P_{out}^1 = \frac{P_{out,N}^1}{1 - P_{rep,N}^1} \tag{26}$$

Therefore, the NARL for the shifted process, is defined as:

$$ARL_{1N} = \frac{1}{P_{out}^1}; ARL_{1N} \in [ARL_{1L}, ARL_{1U}] \tag{27}$$

Table 1 and Table 2 present the results for  $a_N \in [3,5]$ ,  $b_N \in [1.9,2.1]$  and  $a_N \in [5,10]$ ,  $b_N \in [1.45, 1.55]$ , including NARL values for different shifts ranging from 1.0 to 4.0.

**Table 1:** NARL with  $a_N \in [3,5]$  and  $b_N \in [1.9,2.1]$

	Lower	Upper	Lower	Upper	Lower	Upper
$ka_N$	4.5948	5.2333	5.4302	5.4302	5.0009	5.4097
$kr_N$	1.5279	2.8818	0.32429	2.662	0.9223	4.0603
$a_N$	3	5	3	5	3	5
$b_N$	1.9	2.1	1.9	2.1	1.9	2.1
$c$	NARL					
1.0	200	200.01	300.01	300	370	370
1.1	80.02	86.99	101.62	111.28	138.84	149.4
1.2	37.51	43.40	41.19	48.86	61.11	71.14
1.3	19.92	24.14	19.33	24.49	30.54	38.39
1.4	11.71	14.68	10.28	13.69	16.95	22.84
1.5	7.50	9.62	6.11	8.4	10.29	14.7
1.6	5.18	6.72	4.01	5.58	6.75	10.1
1.7	3.81	4.96	2.88	3.99	4.75	7.32]
1.8	2.97	3.85	2.23	3.03	3.55	5.56
1.9	2.42	3.11	1.84	2.43	2.80	4.39
2.0	2.05	2.60	1.59	2.03	2.31	3.58
2.3	1.55	1.88	1.28	1.51	1.66	2.44
2.5	1.32	1.54	1.15	1.29	1.37	1.88
2.8	1.18	1.33	1.08	1.16	1.21	1.53
3.0	1.13	1.25	1.06	1.11	1.15	1.39
4.0	1.03	1.08	1.01	1.03	1.04	1.12

**Table 2:** NARL with  $a_N \in [5,10]$ ,  $b_N \in [1.45, 1.55]$

	Lower	Upper	Lower	Upper	Lower	Upper
$ka_N$	4.0062	4.5711	3.9398	4.7884	4.1479	4.8673
$kr_N$	1.0866	2.2000	2.9391	1.8184	1.4145	1.7991
$a_N$	5	10	5	10	5	10
$b_N$	1.45	1.55	1.45	1.55	1.45	1.55
$c$	NARL					
1.0	200	200	300	300.01	370	370.02
1.1	58.89	72.91	77.12	125.12	91.79	130.98
1.2	21.72	31.51	25.26	61.28	29.13	55.15
1.3	9.65	15.64	10.15	33.91	11.36	26.64
1.4	5.06	8.74	4.93	20.64	5.36	14.42
1.5	3.09	5.42	2.87	13.56	3.04	8.60
1.6	2.15	3.68	1.97	9.48	2.04	5.60
1.7	1.68	2.72	1.53	6.98	1.57	3.93

1.8	1.42	2.15	1.31	5.37	1.33	2.95
1.9	1.27	1.79	1.19,	4.29	1.20	2.35
2.0	1.18	1.57	1.12	3.54	1.12	1.96
2.3	1.07	1.27	1.04	2.45	1.04	1.46
2.5	1.03	1.15	1.02	1.90	1.02	1.25
2.8	1.01	1.08	1.01	1.56	1.01	1.13
3.0	1.01	1.05	1	1.42	1	1.09
4.0	1	1.01	1	1.13	1	1.02

Table 1 presents the NARL values for an in-control state with  $NARL_0 = 200, 300$  and  $370$ . The corresponding values of  $ka_N$  are  $[4.594878, 5.233344]$ ,  $[5.282686, 5.430229]$  and  $[5.000939, 5.409798]$  while  $kr_N$  values are  $[1.527915, 2.881848]$ ,  $[0.3242994, 2.66222]$  and  $[0.9223276, 4.060355]$ . Figure 1 illustrates the plotting for  $a_N \in [3,5]$  and  $b_N \in [1.9,2.1]$ .

From Tables 1-2, we note the following trends in NARL.

1. As the shift value  $c$  increases from 1.0 to 4.0, the indeterminacy intervals  $ARL_{1N} \in [ARL_{1L}, ARL_{1U}]$  decrease.
2. As  $a_N \in [a_L, a_U]$  and  $b_N \in [b_L, b_U]$  increase from  $a_N \in [3,5]$  and  $b_N \in [1.9,2.1]$  to  $a_N \in [5,10]$  and  $b_N \in [1.45, 1.55]$ , the indeterminacy intervals decrease.

### 4 Comparative Study

In this section, we examine the comparative benefits and effectiveness of the proposed chart in relation to the traditional gamma distribution chart within an indeterminacy environment, using simulated data. To ensure a fair comparison, we maintained consistent values for the process parameters. Table 3 presents the in-control  $NARL_0$  and out-of-control  $NARL_1$  values for various shift magnitudes ranging from 1.0 to 4.0.

**Table 3:** NARL of two charts

Existing		Proposed		Existing		Proposed	
Lower	Upper	Lower	Upper	Lower	Upper	Lower	Upper
300	300	300	300	370.01	370.01	370	370
128.2	146.3	101.62	111.28	154.21	176.4	138.84	149.4
64.73	81.41	41.19	48.86	76.20	96.30	61.11	71.14
37.02	50.05	19.33	24.49	42.82	58.27	30.54	38.39
23.32	33.26	10.28	13.69	26.57	38.20	16.95	22.84
15.84	23.51	6.11	8.40	17.82	26.68	10.29	14.70
11.43	17.45	4.01	5.58	12.72	19.61	6.75	10.1
8.66	13.49	2.88	3.99	9.54	15.02	4.75	7.32
6.83	10.77	2.23	3.03	7.46	11.90	3.55	5.56
5.56	8.85	1.84	2.43	6.03	9.70	2.80	4.39

4.65	7.43	1.59	2.03	5.01	8.10	2.31	3.58
3.27	5.21	1.28	1.51	3.47	5.61	1.66	2.44
2.53	3.97	1.15	1.29	2.66	4.23	1.37	1.88
2.02	3.10	1.08	1.16	2.10	3.27	1.21	1.53
1.81	2.72	1.06	1.11	1.87	2.85	1.15	1.39
1.31	1.79	1.01	1.03	1.33	1.85	1.04	1.12

A straightforward comparison reveals that the proposed chart exhibits lower  $NARL_1$  values compared to the existing chart by Aslam et al [43]. For instance, when  $c = 1.1$ , the lower NARL is 154.21 from the existing chart and it is 138.84 from the proposed control chart.

### 5 Simulation Study

We will now evaluate the efficiency of the proposed control chart compared to the existing chart using simulated data. The first twenty values are generated from the neutrosophic gamma distribution assuming in-control process and twenty more values from the shifted process when  $c=1.4$ . The values of  $T_N^*$  are computed and plotted on Figure 1, while the existing control chart is shown in Figure 2. Based on Table 1, a shift should be noticeable between the 16th and 22nd samples. Figure 1 illustrates the performance of the proposed control chart, with the determined part (lower value) of the statistic  $T_N^*$  surpassing  $UCL_{1N}$  between the 16th and 22nd samples. Additionally, several observations fall within the indeterminacy interval and resampling regions. In contrast, the current control chart does not show any shift in the process. This simulation study highlights that the proposed control chart is more efficient at detecting process shifts compared to the existing chart.

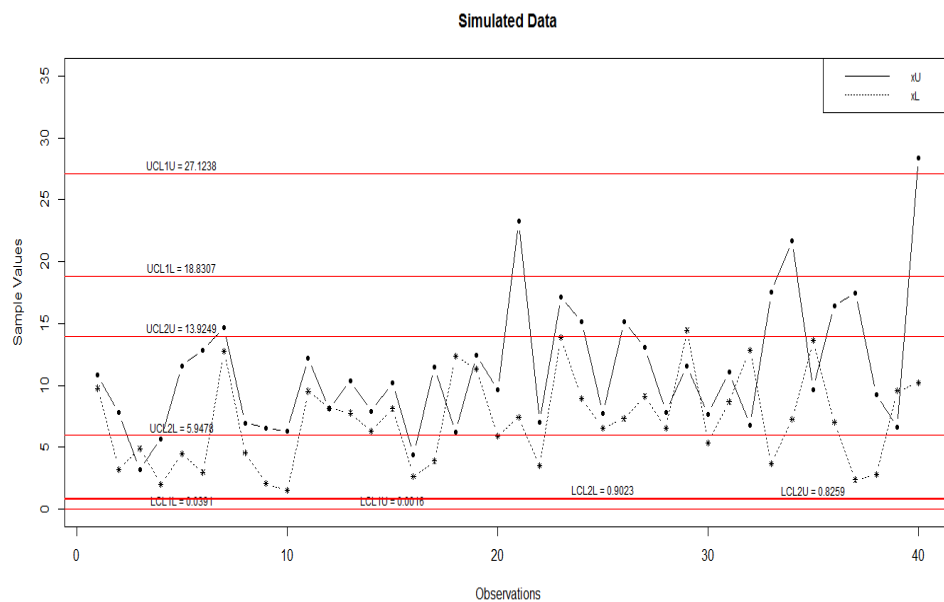


**Figure 1:** The proposed control for simulated data

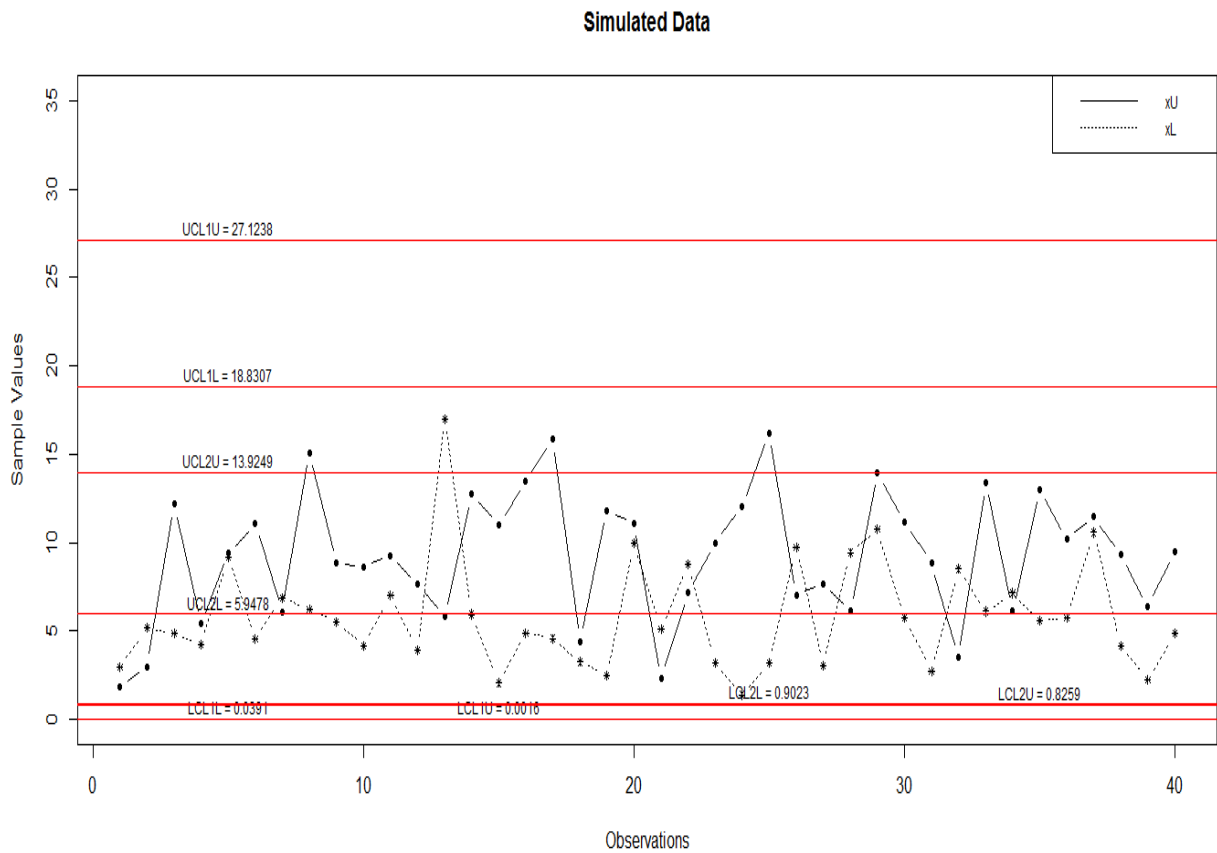


**Figure 2:** The existing control chart for simulated data

### 6. Application of the Proposed Chart

In this section, we delve into the implementation of the proposed control chart in the healthcare field. A prominent hospital is interested in tracking urinary tract infections (UTIs) among patients. As highlighted by Santiago and Smith [44], “data were provided by a large hospital system with concerns about a high rate of hospital-acquired UTIs.” Specifically, the hospital aims to monitor the frequency of UTIs acquired during hospital stays to swiftly identify increases in infection rates or evaluate whether changes in processes or materials lead to fewer infections. The root causes often vary by gender, affecting both male and female patients. Data on UTIs in male patients, obtained from Aslam et al [43] and Almarashi and Aslam [45], is shown in Table 4. Given that the UTI data is presented in intervals, the existing control chart proposed by Santiago and Smith [44] is not suitable for monitoring UTIs. Instead, the hospital management can use the proposed control chart for this purpose. For instance, with  $ARL_{0N} \in [370, 370]$ ,  $a_N \in [7.6666, 7.7777]$ ,  $b_N \in [1.0959, 1.1559]$ , and  $n_N \in [50, 50]$ , the control limit coefficients are  $k_{1N} \in [3.3590, 3.7703]$  and  $k_{2N} \in [0.1637, 2.0479]$ . Figure 3 presents the proposed control chart for monitoring UTI patients. The chart indicates that two points exceed the upper control limits. In contrast, the control chart from Aslam et al [43] shows that all data points stay within the control limits. Additionally, the proposed chart highlights several points within the indeterminacy interval and repetitive regions. This suggests that hospital management may need to re-evaluate certain observations within these intervals and consider repeating the process for those cases. Comparing the proposed UTI control

chart with the one by Aslam et al [43], it is clear that the proposed chart provides a more distinct indication of potential issues in tracking UTI patients, prompting the need for corrective actions to bring the process back to a controlled state. This method can be similarly applied to other datasets.

**Table 4: The Neutrosophic UTIs data**

Sr#	$T_N$	$T_N^*$	Sr#	$T_N$	$T_N^*$
1	[13.13,13.56]	[2.35,2.38]	26	[6.53,12.47]	[1.87,2.31]
2	[3.57,15.55]	[1.52,2.49]	27	[6.85,12.13]	[1.89,2.29]
3	[4.31,16.50]	[1.62,2.54]	28	[8.08,22.69]	[2.00,2.83]
4	[2.76,25.53]	[1.40,2.94]	29	[11.61,17.14]	[2.26,2.57]
5	[7.75,15.38]	[1.97,2.48]	30	[3.98,17.16]	[1.58,2.57]
6	[11.45,13.18]	[2.25,2.36]	31	[6.81,17.25]	[1.89,2.58]
7	[9.20,15.18]	[2.09,2.47]	32	[4.42,12.53]	[1.64,2.32]
8	[5.51,9.77]	[1.76,2.13]	33	[6.53,13.96]	[1.86,2.40]
9	[8.18,13.07]	[2.01,2.35]	34	[8.73,9.30]	[2.05,2.10]
10	[7.07,19.91]	[1.91,2.71]	35	[5.37,9.43]	[1.75,2.11]
11	[7.35,14.89]	[1.94,2.46]	36	[8.44,6.35]	[2.03,1.85]
12	[5.62,11.09]	[1.77,2.23]	37	[11.79,17.01]	[2.27,2.57]
13	[8.38,16.72]	[2.03,2.55]	38	[5.33,14.90]	[1.74,2.46]
14	[9.49,10.06]	[2.11,2.15]	39	[4.20,21.20]	[1.61,2.76]
15	[4.90,23.67]	[1.69,2.87]	40	[5.74,11.95]	[1.79,2.28]
16	[4.45,14.68]	[1.64,2.44]	41	[5.24,11.09]	[1.73,2.23]
17	[7.11,16.44]	[1.92,2.54]	42	[5.10,10.10]	[1.72,2.16]
18	[9.37,15.95]	[2.10,2.51]	43	[9.11,24.54]	[2.08,2.90]
19	[12.00,16.38]	[2.28,2.53]	44	[8.39,10.21]	[2.03,2.16]
20	[7.41,16.62]	[1.95,2.55]	45	[5.33,18.03]	[1.74,2.62]
21	[10.64,15.15]	[2.19,2.47]	46	[7.90,11.43]	[1.99,2.25]
22	[6.63,11.21]	[1.87,2.23]	47	[3.62,13.00]	[1.53,2.35]
23	[2.87,14.27]	[1.42,2.42]	48	[5.01,13.62]	[1.71,2.38]
24	[6.87,10.37]	[1.90,2.18]	49	[4.09,12.88]	[1.60,2.34]
25	[6.16,18.85]	[1.83,2.66]	50	[9.38,17.45]	[2.10,2.59]

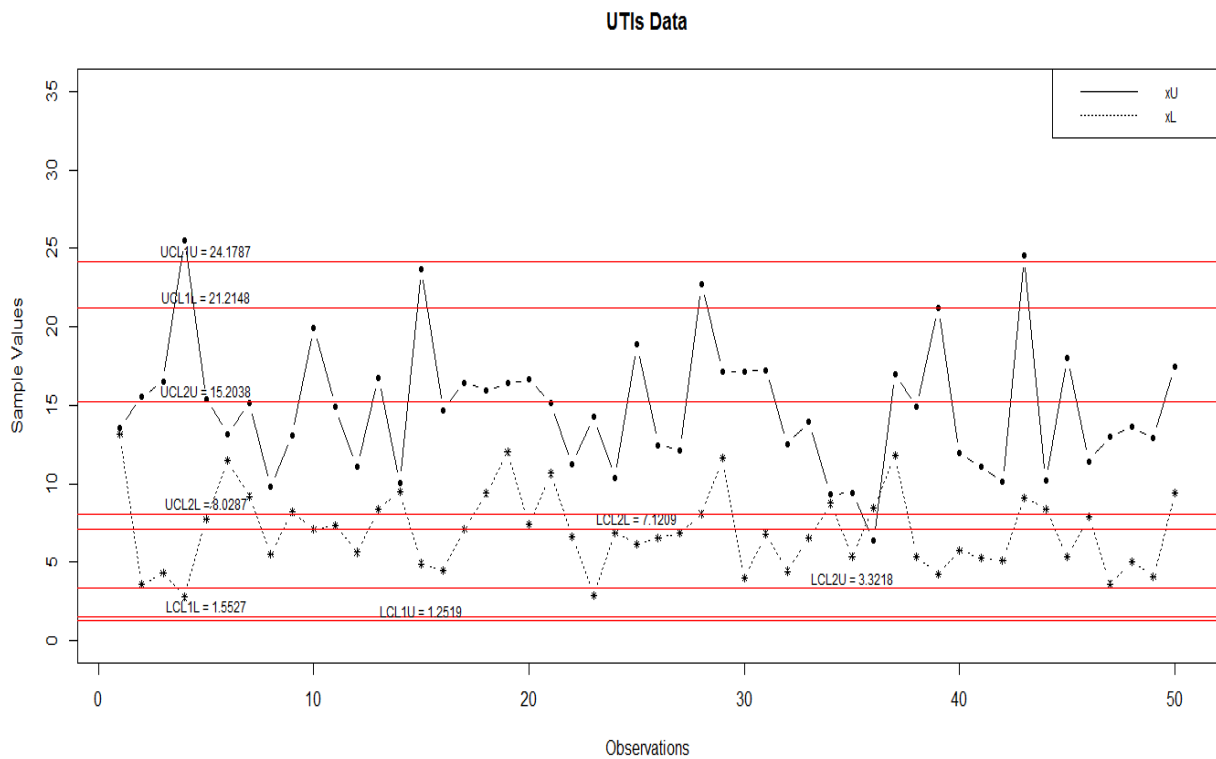


**Figure 3:** The proposed control chart for UTIs patients

## 7. Concluding Remarks

In this article, we introduced a control chart based on repetitive sampling within the framework of neutrosophic statistics, specifically for data following a gamma distribution. We provided essential metrics to evaluate the effectiveness of the proposed control chart. To demonstrate its efficacy, we included both a simulation study and a real-world example from healthcare. The findings indicate that the proposed chart is a valuable addition to the quality control toolkit. Future research could extend this work to multivariate cases and explore its application with different transformations for non-normal distributions and diverse datasets. Additionally, investigating the control chart using cost models and its potential for monitoring imbalanced data are promising avenues for future research.

**Acknowledgments:** The authors are deeply thankful to the editor and reviewers for their valuable suggestions to improve the quality and presentation of the paper.

## References

- [1] G. Suman and D. Prajapati, "Control chart applications in healthcare: a literature review," *Int. J. Metrol. Qual. Eng.*, vol. 9, p. 5, 2018.

- [2] B. Zaman, M. H. Lee, and M. Riaz, "An improved process monitoring by mixed multivariate memory control charts: An application in wind turbine field," *Comput. Ind. Eng.*, vol. 142, p. 106343, 2020.
- [3] M. P. Hossain, M. H. Omar, M. Riaz, and S. Y. Arafat, "On designing a new control chart for Rayleigh distributed processes with an application to monitor glass fiber strength," *Commun. Stat. Comput.*, vol. 51, no. 6, pp. 3168–3184, 2022.
- [4] D. C. Montgomery, *Introduction to statistical quality control*. John Wiley & Sons, 2019.
- [5] L. Ahmad, M. Aslam, and C.-H. Jun, "The design of a new repetitive sampling control chart based on process capability index," *Trans. Inst. Meas. Control*, vol. 38, no. 8, pp. 971–980, 2016.
- [6] W. A. Shewhart, "Quality control charts," *Bell Syst. Tech. J.*, vol. 5, no. 4, pp. 593–603, 1926.
- [7] M. Abid, H. Z. Nazir, M. Tahir, M. Riaz, and T. Abbas, "A comparative analysis of robust dispersion control charts with application related to health care data," *J. Test. Eval.*, vol. 48, no. 1, pp. 247–259, 2020, doi: 10.1520/JTE20180572.
- [8] M. Aslam and M. A. Raza, "Design of new sampling plans for multiple manufacturing lines under uncertainty," *Int. J. Fuzzy Syst.*, vol. 21, pp. 978–992, 2019.
- [9] H. Z. Nazir, T. Hussain, N. Akhtar, M. Abid, and M. Riaz, "Robust adaptive exponentially weighted moving average control charts with applications of manufacturing processes," *Int. J. Adv. Manuf. Technol.*, vol. 105, pp. 733–748, 2019.
- [10] A. Saghir, L. Ahmad, and M. Aslam, "Modified EWMA control chart for transformed gamma data," *Commun. Stat. Comput.*, vol. 50, no. 10, pp. 3046–3059, 2021.
- [11] R. E. Sherman, "Design and evaluation of a repetitive group sampling plan," *Technometrics*, vol. 7, no. 1, pp. 11–21, 1965.
- [12] S. Balamurali, H. Park, C.-H. Jun, K.-J. Kim, and J. Lee, "Designing of variables repetitive group sampling plan involving

- minimum average sample number," *Commun. Stat. Comput.*, vol. 34, no. 3, pp. 799–809, 2005.
- [13] D. K. Bhaumik and R. D. Gibbons, "One-sided approximate prediction intervals for at least  $p$  of  $m$  observations from a gamma population at each of  $r$  locations," *Technometrics*, vol. 48, no. 1, pp. 112–119, 2006.
- [14] L. Ahmad, M. Aslam, and C.-H. Jun, "Coal quality monitoring with improved control charts," *Eur. J. Sci. Res.*, vol. 125, no. 2, pp. 427–434, 2014.
- [15] M. Azam, O. H. Arif, M. Aslam, and W. Ejaz, "Repetitive acceptance sampling plan based on exponentially weighted moving average regression estimator," *J. Comput. Theor. Nanosci.*, vol. 13, no. 7, pp. 4413–4426, 2016.
- [16] H. A. Al-Oraini and M. A. Rahim, "Economic statistical design of  $X$  control charts for systems with Gamma  $(\lambda, 2)$  in-control times," *Comput. Ind. Eng.*, vol. 43, no. 3, pp. 645–654, 2002.
- [17] Z. G. B. Stoumbos and M. R. Reynolds Jr, "Robustness to non-normality and autocorrelation of individuals control charts," *J. Stat. Comput. Simul.*, vol. 66, no. 2, pp. 145–187, 2000.
- [18] H. Aksoy, "Use of gamma distribution in hydrological analysis," *Turkish J. Eng. Environ. Sci.*, vol. 24, no. 6, pp. 419–428, 2000.
- [19] A. Saghir, L. Ahmad, M. Aslam, and C.-H. Jun, "A EWMA control chart based on an auxiliary variable and repetitive sampling for monitoring process location," *Commun. Stat. Comput.*, vol. 48, no. 7, pp. 2034–2045, 2019.
- [20] M. Aslam, N. Khan, and C.-H. Jun, "A control chart using belief information for a gamma distribution," *Oper. Res. Decis.*, vol. 26, no. 4, pp. 5–19, 2016.
- [21] D. Jearkpaporn, D. C. Montgomery, G. C. Runger, and C. M. Borrer, "Process monitoring for correlated gamma-distributed data using generalized-linear-model-based control charts," *Qual. Reliab. Eng. Int.*, vol. 19, no. 6, pp. 477–491, 2003.
- [22] C. W. Zhang, M. Xie, J. Y. Liu, and T. N. Goh, "A control chart for

- the Gamma distribution as a model of time between events," *Int. J. Prod. Res.*, vol. 45, no. 23, pp. 5649–5666, 2007.
- [23] F. L. Chen and C.-H. Yeh, "Economic statistical design of non-uniform sampling scheme  $\bar{X}$  bar control charts under non-normality and Gamma shock using genetic algorithm," *Expert Syst. Appl.*, vol. 36, no. 5, pp. 9488–9497, 2009.
- [24] I. M. Gonzalez and E. Viles, "Design of R control chart assuming a gamma distribution," 2001.
- [25] C. W. Bradshaw Jr, "A fuzzy set theoretic interpretation of economic control limits," *Eur. J. Oper. Res.*, vol. 13, no. 4, pp. 403–408, 1983.
- [26] R. H. Williams and R. M. Zigli, "Ambiguity impedes quality in the service industries," *Qual. Prog.*, vol. 20, no. 7, pp. 14–17, 1987.
- [27] H. Taleb and M. Limam, "On fuzzy and probabilistic control charts," *Int. J. Prod. Res.*, vol. 40, no. 12, pp. 2849–2863, 2002.
- [28] M. Gülbay, C. Kahraman, and D. Ruan, " $\alpha$ -Cut fuzzy control charts for linguistic data," *Int. J. Intell. Syst.*, vol. 19, no. 12, pp. 1173–1195, 2004.
- [29] K.-L. Hsieh, L.-I. Tong, and M.-C. Wang, "The application of control chart for defects and defect clustering in IC manufacturing based on fuzzy theory," *Expert Syst. Appl.*, vol. 32, no. 3, pp. 765–776, 2007.
- [30] J. Chen, J. Ye, and S. Du, "Scale effect and anisotropy analyzed for neutrosophic numbers of rock joint roughness coefficient based on neutrosophic statistics," *Symmetry (Basel)*, vol. 9, no. 10, p. 208, 2017.
- [31] M. Aslam, "A new sampling plan using neutrosophic process loss consideration," *Symmetry (Basel)*, vol. 10, no. 5, p. 132, 2018.
- [32] W. E. Molnau, G. C. Runger, D. C. Montgomery, K. R. Skinner, E. N. Loreda, and S. S. Prabhu, "A program for ARL calculation for multivariate EWMA charts," *J. Qual. Technol.*, vol. 33, no. 4, pp. 515–521, 2001.
- [33] J. R. Schaffer and M.-J. Kim, "Number of replications required in

- control chart Monte Carlo simulation studies," *Commun. Stat. Comput.*, vol. 36, no. 5, pp. 1075–1087, 2007.
- [34] S. Knoth, "Accurate ARL calculation for EWMA control charts monitoring normal mean and variance simultaneously," *Seq. Anal.*, vol. 26, no. 3, pp. 251–263, 2007.
- [35] Z. Li, C. Zou, Z. Gong, and Z. Wang, "The computation of average run length and average time to signal: an overview," *J. Stat. Comput. Simul.*, vol. 84, no. 8, pp. 1779–1802, 2014.
- [36] C. Chananet, S. Sukparungsee, and Y. Areepong, "The ARL of EWMA chart for monitoring ZINB model using Markov chain approach," *Int. J. Appl. Phys. Math.*, vol. 4, no. 4, p. 236, 2014.
- [37] S. Phanyaem, Y. Areepong, and S. Sukparungsee, "Numerical integration of average run length of CUSUM control chart for ARMA process," *Int. J. Appl. Phys. Math.*, vol. 4, no. 4, p. 232, 2014.
- [38] M. Aslam, O.-H. Arif, and C.-H. Jun, "A control chart for gamma distribution using multiple dependent state sampling," *Ind. Eng. Manag. Syst.*, vol. 16, no. 1, pp. 109–117, 2017.
- [39] E. B. Wilson and M. M. Hilferty, "The distribution of chi-square," *Proc. Natl. Acad. Sci.*, vol. 17, no. 12, pp. 684–688, 1931.
- [40] X. Peng and J. Dai, "Approaches to single-valued neutrosophic MADM based on MABAC, TOPSIS and new similarity measure with score function," *Neural Comput. Appl.*, vol. 29, pp. 939–954, 2018.
- [41] X. Peng and J. Dai, "A bibliometric analysis of neutrosophic set: two decades review from 1998 to 2017," *Artif. Intell. Rev.*, vol. 53, no. 1, pp. 199–255, 2020.
- [42] S. Sheu and T. Lin, "The generally weighted moving average control chart for detecting small shifts in the process mean," *Qual. Eng.*, vol. 16, no. 2, pp. 209–231, 2003.
- [43] M. Aslam, G. S. Rao, A. H. AL-Marshadi, L. Ahmad, and C.-H. Jun, "Control charts for monitoring process capability index using median absolute deviation for some popular distributions," *Processes*, vol. 7, no. 5, p. 287, 2019.

- [44] E. Santiago and J. Smith, "Control charts based on the exponential distribution: Adapting runs rules for the t chart," *Qual. Eng.*, vol. 25, no. 2, pp. 85–96, 2013.
- [45] A. M. Almarashi and M. Aslam, "[Retracted] Process Monitoring for Gamma Distributed Product under Neutrosophic Statistics Using Resampling Scheme," *J. Math.*, vol. 2021, no. 1, p. 6635846, 2021.

Received: Aug 5, 2024. Accepted: Nov 6, 2024